

See discussions, stats, and author profiles for this publication at: <https://www.researchgate.net/publication/50273198>

A Site-Saturated Mutagenesis Study of Pentaerythritol Tetranitrate Reductase Reveals that Residues 181 and 184 Influence Ligand Binding, Stereochemistry and Reactivity

ARTICLE *in* CHEMBIOCHEM · MARCH 2011

Impact Factor: 3.09 · DOI: 10.1002/cbic.201000662 · Source: PubMed

CITATIONS

30

READS

42

8 AUTHORS, INCLUDING:



[Helen S Toogood](#)

The University of Manchester

55 PUBLICATIONS 1,108 CITATIONS

[SEE PROFILE](#)



[Ania Fryszkowska](#)

Dr. Reddy's Laboratories EU Ltd

22 PUBLICATIONS 432 CITATIONS

[SEE PROFILE](#)



[Nigel S Scrutton](#)

The University of Manchester

347 PUBLICATIONS 7,856 CITATIONS

[SEE PROFILE](#)

A Site-Saturated Mutagenesis Study of Pentaerythritol Tetranitrate Reductase Reveals that Residues 181 and 184 Influence Ligand Binding, Stereochemistry and Reactivity

Helen S. Toogood,^{*,[a]} Anna Fryszkowska,^[b] Martyn Hulley,^[a] Michiyo Sakuma,^[a] David Mansell,^[b] Gill M. Stephens,^[c] John M. Gardiner,^[b] and Nigel S. Scrutton^{*,[a]}

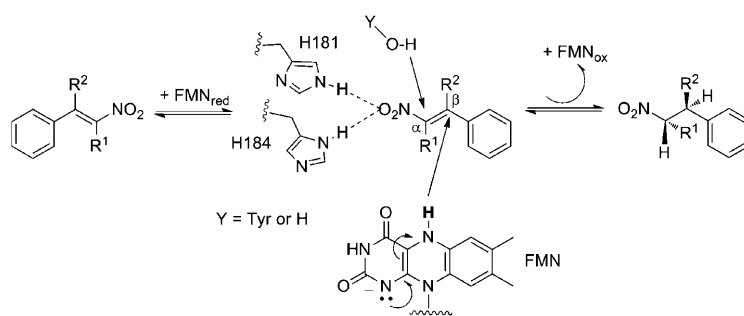
We have conducted a site-specific saturation mutagenesis study of H181 and H184 of flavoprotein pentaerythritol tetranitrate reductase (PETN reductase) to probe the role of these residues in substrate binding and catalysis with a variety of α,β -unsaturated alkenes. Single mutations at these residues were sufficient to dramatically increase the enantiopurity of products formed by reduction of 2-phenyl-1-nitropropene. In addition, many mutants exhibited a switch in reactivity to predominantly catalyse nitro reduction, as opposed to C=C reduction. These mutants showed an enhancement in a minor side

reaction and formed 2-phenylpropanal oxime from 2-phenyl-1-nitropropene. The multiple binding conformations of hydroxy substituted nitro-olefins in PETN reductase were examined by using both structural and catalytic techniques. These compounds were found to bind in both active and inhibitory complexes; this highlights the plasticity of the active site and the ability of the H181/H184 couple to coordinate with multiple functional groups. These properties demonstrate the potential to use PETN reductase as a scaffold in the development of industrially useful biocatalysts.

Introduction

The use of biocatalysts in asymmetric synthesis has become an increasingly cost effective and established manufacturing technique in the production of fine chemicals, pharmaceuticals and agrochemical intermediates.^[1,2] Asymmetric reduction of activated C=C bonds is an attractive way of introducing up to two stereogenic centres into a molecule, and has received a lot of attention in the literature.^[1,3] The usefulness of biocatalysts, such as whole cell preparations and purified enzymes, is due to the often unmatched high efficiency, chemo-, regio- and stereoselectivity of enzyme catalysed reactions.^[2,4] However, naturally occurring biocatalysts can lack some properties necessary in large scale chemical synthesis, such as high activity and selectivity for non-natural substrates.^[5]

The OYE family of enzymes (OYE; E.C. 1.6.99.1) are an extensively characterised group of flavoprotein oxidoreductases capable of catalysing the asymmetric reduction of a variety of activated α,β -unsaturated alkenes.^[1] These FMN-containing, NAD(P)H-dependent oxidoreductases catalyse the reduction of α,β -unsaturated aldehydes, ketones, nitroalkenes, carboxylic acids and derivatives (Scheme 1) to yield products with a variety of biotechnological and pharmaceutical applications.^[6–9] Members of this family are found in yeast, bacteria and plants including the enzymes OYE1 (brewers' yeast),^[10] pentaerythritol tetranitrate reductase (PETN reductase; *Enterobacter cloacae* PB2),^[11] YqjM (*Bacillus subtilis*),^[12] SYE1 (*Shewanella oneidensis*),^[13] OPR1-2 (*Arabidopsis thaliana*),^[14] morphinone reductase (MR; *Pseudomonas putida*)^[15] and a thermostable family member TOYE (*Thermoanaerobacter pseudethanolicus* E39).^[16]



Scheme 1. General mechanism and stereochemistry of nitroalkene reduction by PETN reductase; R¹, R²: CH₃ or H.

Improvements in key characteristics of enzymes, such as substrate binding, stereo- and enantioselectivity of substrates

[a] Dr. H. S. Toogood, M. Hulley, M. Sakuma, Prof. N. S. Scrutton
Faculty of Life Sciences, University of Manchester
131 Princess Street, Manchester M1 7DN (UK)
Fax: (+44) 161-306-8918
E-mail: helen.toogood@manchester.ac.uk
nigel.scrutton@manchester.ac.uk

[b] Dr. A. Fryszkowska, Dr. D. Mansell, Dr. J. M. Gardiner
School of Chemistry, University of Manchester
131 Princess Street, Manchester M1 7DN (UK)

[c] Prof. G. M. Stephens
Department of Chemical and Environmental Engineering
University of Nottingham, University Park
Nottingham NG7 2RD (UK)

Supporting information for this article is available on the WWW under <http://dx.doi.org/10.1002/cbic.201000662>.

and/or products, and even increasing the biocatalyst stability under industrial reaction conditions (e.g., towards high organic solvent content) are often necessary in the realisation of the industrial potential of any biocatalyst.^[17,18] A recent review of the biocatalytic potential of the OYE family in the reduction of a diverse range of industrially useful activated compounds highlighted the importance of understanding the three dimensional enzyme structural information and its role in directing the stereochemical course of substrate reduction. This information is invaluable in guiding a rational approach to engineering more useful biocatalysts by site-directed mutagenesis.^[11]

We recently screened single site-saturated libraries of PETN reductase active site residues T26X, Y68X, W102X, H181X, H184X, Q241X and Y351X to identify mutants with improved biocatalytic potential.^[19] The highly conserved active site couple H181 and H(N)184 (PETN reductase numbering) is known to play a pivotal role in both reductive and oxidative substrate binding.^[16,20–23] In addition, these residues are known to be key in the formation of a charge-transfer complex (CTC) with phenolic inhibitors by forming hydrogen bonds with the hydroxy substituent of the aromatic ligands.^[21,23–25] The three dimensional crystal structures of OYE1,^[21] MR^[26] and PETN reductase^[22,27,28] revealed the presence of a weak interaction between atoms H181 NE2 and FMN isoalloxazine O2, although this was not present in all structures of these enzymes. Site saturated library screening studies with YqjM did not include mutations at the equivalent residues H164/H167 due to the assumption that these residues participate in the catalytic process.^[29] However, we have previously shown that PETN reductase H181X and H184X site-saturated libraries retain some activity in both the reductive and oxidative half reactions, therefore, these residues do not play an essential role in catalysis.^[19,22]

Here, we investigated the reaction selectivity of site-saturated libraries of H181 and H184 by monitoring the conversion, yields, *ee* values and side-product formation during reduction of a variety of activated alkene substrates. A marked variation in both the yields of C=C reduction and by-product formation (e.g., oxime formation) was observed. There were often dramatic improvements in product enantiopurity in the reactions with 2-aryl-1-nitropropene substrates, and these mutants are discussed in terms of the nature and position of the mutation and possible mechanisms of product formation. To further understand the importance of the H181/H184 couple, we describe the spectroscopic changes upon binding of hydroxy substituted 1-aryl-2-nitroethene and 1-aryl-2-nitropropene ligands to wild-type PETN reductase. The crystal structures of both the H181N and H184N mutants have been determined in addition to three inhibitor-bound wild-type enzyme structures.

Results and Discussion

PETN reductase H181X and H184X library biotransformations

We produced almost all single site-saturated PETN reductase-His₈ H181X and H184X mutants using a combination of both

identification by gene sequencing of random library clones^[19] and site-directed mutagenesis. Each mutant enzyme was expressed in *Escherichia coli* and purified to ~95% by using the affinity resin Ni-IDA. We were unable to generate the mutant H184Q due to a lack of PCR product, whilst mutant H181M was not studied due to a deficiency of significant protein expression.

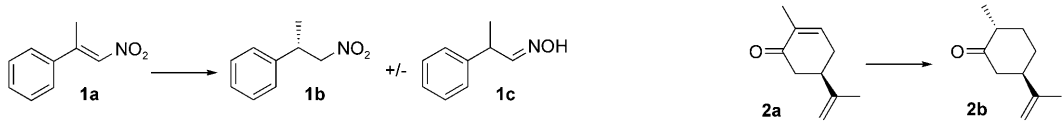
We performed anaerobic biotransformations with wild-type PETN reductase and H181X/H184X mutants to investigate the effect of each of the single amino acid changes at these key active site substrate-binding residues. Reactions with 2-phenyl-1-nitropropene ((*E*)-**1a**) and (5*R*)-carvone (**2a**) were performed by using a NADP⁺/glucose-6-phosphate dehydrogenase (G6PDH) cofactor recycling system or NAD(P)H as the cofactor (Table 1). The wild-type enzyme reduced nitroalkene (*E*)-**1a** to 100% conversion under our reaction conditions to produce the equivalent alkane product (*S*)-**1b** with a moderate *ee* and around 10% of the 2-phenylpropanal oxime by-product, **1c**. Other by-products were also formed and were previously identified as the equivalent aldehyde (2-phenylpropanal) and alcohol (2-phenylpropan-1-ol), the latter likely formed by the reduction of **1d** by an endogenous keto reductase found in the *E. coli* host.^[17–19] All mutants were compromised to some extent in terms of the conversion and/or yields compared to wild-type reactions (Table 1). There was evidence of significant noncatalytic substrate (*E*)-**1a** decomposition under the reaction conditions in the case of low conversions (up to 50%). However, this was less evident when significant substrate reduction was present (results not shown).

Notably, all H181X mutants showed >70% decrease in alkane product yields by using the NADP⁺/G6PDH recycling system. This is in contrast to the H184X library that had fewer mutants with dramatic reductions in catalytic activity (H184D/E/I/L/V/W). However, this effect was less evident when using NADH as the cofactor (Table 1 and Table S1 in the Supporting Information; data in parentheses). In addition, the majority of the H184X mutants showed similar or lower levels of oxime formation compared to the wild-type enzyme.

To our surprise, the majority of the H181X/H184X mutants showed a dramatic increase in the enantiopurity of the alkane product enantiopurity (>80%) compared to wild-type enzyme. In many cases this was concomitant with an increase in the yield of oxime by-product formation (up to 75%), especially in the case of the H181X library (Table 1 and Table S1 in the Supporting Information; NADP⁺/G6PDH recycling system). Some mutants generated almost optically pure (*S*)-**1b** (H181I/N and H184R/T), while mutant H184Y showed a more moderate increase in *ee* (75%). In contrast, mutants H184K and H184R produced moderate yields of (*S*)-**1b** to high enantiopurity but with lower oxime production than the wild-type enzyme. Therefore, this single residue change altered the reaction selectivity of the enzyme in favour of nitro reduction to form the oxime product, making (*S*)-**1b** formation the “side-product”.

The introduction of a novel activity into an enzyme is often considered to be quite demanding due to the need to identify and precisely position new functional groups necessary for successful catalysis.^[30] However, we have shown in this work

Table 1. Reduction of 2-aryl-1-nitropropene ((*E*)-**1a**) and carvone (5*R*)-**2a** by wild-type and mutant PETN reductases.^[a]

									
Mutant	Conv. ^[b,c] [%]	Yield ^[c] [%]	ee ^[d] [%]	Config.	Oxime ^[c] [%]	Conv. ^[b,c] [%]	Yield ^[c] [%]	de ^[d] [%]	Config.
wild type	> 99 (88)	70 (62)	42 (54)	<i>S</i>	10 (9)	> 99	76	94	2 <i>R</i> ,5 <i>R</i>
H181A	86 (91)	9 (5)	92 (82)	<i>S</i>	75 (21)	48	29	89	2 <i>R</i> ,5 <i>R</i>
H181C	79 (72)	4 (3)	> 85 (63)	<i>S</i>	67 (19)	9	5	77	2 <i>R</i> ,5 <i>R</i>
H181T	84 (86)	5 (3)	> 5 (69)	<i>S</i>	58 (20)	38	28	89	2 <i>R</i> ,5 <i>R</i>
H181N	83 (85)	20 (13)	94 (88)	<i>S</i>	52 (15)	23	17	75	2 <i>R</i> ,5 <i>R</i>
H181R	< 5 (31)	< 2 (3)	n.d. (15)	<i>S</i>	0 (0)	< 2	< 2	–	n.d.
H181W	< 5 (23)	< 2 (< 2)	n.d. (n.d.)	<i>S</i>	0 (4)	< 2	< 2	–	n.d.
H181Y	< 5 (15)	< 2 (2)	n.d. (n.d.)	<i>S</i>	0 (0)	< 2	< 2	–	n.d.
H184F	24 (82)	5 (4)	> 85 (57)	<i>S</i>	19 (11)	22	14	92	2 <i>R</i> ,5 <i>R</i>
H184N	84 (83)	67 (60)	85 (87)	<i>S</i>	17 (4)	> 99	70	95	2 <i>R</i> ,5 <i>R</i>
H184A	75 (73)	47 (21)	90 (89)	<i>S</i>	17 (8)	51	26	85	2 <i>R</i> ,5 <i>R</i>
H184D	< 5 (47)	< 2 (3)	n.d. (51)	<i>S</i>	0 (1)	< 2	< 2	–	n.d.
H184E	< 5 (53)	< 2 (1)	n.d. (25)	<i>S</i>	2 (1)	< 2	< 2	–	n.d.
H184I	< 5 (60)	3 (4)	> 85 (70)	<i>S</i>	4 (3)	18	< 2	–	n.d.
H184K	34 (77)	36 (25)	82 (80)	<i>S</i>	7 (3)	< 2	< 2	–	n.d.
H184L	< 5 (46)	< 2 (3)	n.d. (51)	<i>S</i>	1 (3)	< 2	< 2	–	n.d.
H184R	65 (65)	38 (35)	94 (91)	<i>S</i>	3 (1)	< 1	< 2	–	n.d.
H184V	< 5 (68)	< 2 (4)	n.d. (65)	<i>S</i>	1 (5)	< 2	< 2	–	n.d.
H184W	< 5 (54)	< 2 (5)	n.d. (59)	<i>S</i>	3 (3)	10	5	94	2 <i>R</i> ,5 <i>R</i>

[a] Reactions (1 mL) contained alkene (5 mM; added as a 2% DMF solution), NADH (10 mM) and PETN reductase (4 or 10 μM) and were incubated at 30 °C for 4 h at 130 rpm. Reactions with the NADP⁺/G6PDH recycling system (1.0 mL) were performed in buffer (50 mM KH₂PO₄/K₂HPO₄, pH 7.0) containing alkene (5 mM; added as a 2% DMF solution), NADP (6 μM), glucose-6-phosphate (10 mM), glucose-6-phosphate dehydrogenase (8 U) and PETN reductase (2 μM) and were incubated at 30 °C for 48 h at 130 rpm. Reactions in the presence of NADH are shown in parentheses. The results of the remaining mutants can be found in Table S1 in the Supporting Information. [b] Conv.: % conversion; [c] yield of the equivalent alkane product determined by GC by using a DB-Wax column; [d] Determined by either GC (DB-Wax column; **2a**) or HPLC (Chiralcel OD column) as described in the Experimental Section. Side-products of **1a** reduction to form the equivalent aldehyde by-product were detected with some mutants in reactions in the presence of NADH (H181A/S/G/V/L/I/T/C) and (H184F/G/A). However, the levels were < 10% in all cases. Conv.: % conversion is defined as the loss of substrate due to enzymatic reduction and noncatalytic decomposition; Config.: configuration; n.d.: not determined.

the enhancement of a minor promiscuous side reaction(s) at the expense of the predominant wild-type-like biotransformation, which in effect mimics divergent evolution.^[31] Active or binding site residues important for functional plasticity were identified and subjected to rounds of mutagenesis. This method has also been used successfully in the generation of seven highly specific and catalytically distinct mutants of γ -humulene synthase, whereas the wild type is nonselective and produces 52 different sesquiterpenes from farnesyl diphosphate.^[32]

A number of mutants had severely compromised activity and showed almost no alkane or oxime formation (H181R/W/Y and H184D/E/I/L/V/W). Interestingly, the majority of these mutants had amino acid substitutions that were hydrophobic and/or bulky. As residues H181 and H184 play a pivotal role in substrate binding,^[16,20–23] this suggests that the presence of a bulky and/or hydrophobic group in this position compromises ligand binding, and therefore, reduces the overall catalytic rate. However, H181 and H184 are also thought to play a role in increasing the electron withdrawing ability of the substrate activating group (e.g., nitro group),^[22] which could also impact on the catalytic rate. Therefore, the poor activity of the H184D/E mutants might be due to the substitution of the positively

charged histidine to negatively charged residues, which likely effects the binding of the electronegative nitro group of the substrate. As these residues are also important for binding the reductive substrates, NAD(P)H binding could also be compromised.^[22] Further detailed kinetic studies are required to determine the relative contributions of alteration in substrate binding and/or reduction in substrate activation in effecting (*E*)-**1a** reduction by these mutants.

Some mutants showing only minor decreases in substrate conversion showed a significant increase in the levels of oxime formation and concomitant decrease in alkane yield (e.g., H181C and H184N). In contrast some mutants showed poor conversions and low levels of oxime formation, such as H181F/K and H184C/K/P (Table 1 and Table S1 in the Supporting Information). However, the high conversions are likely a reflection of the increased rate of oxime formation as opposed to significant differences in the level of alkane product formation, which is typically low in most of these mutants. Only three H181X mutants showed severe reductions in substrate conversion (H181R/W/Y), all of which contain large charged or hydrophobic functional groups close to the FMN (Table 1).

Previous modelling and biotransformation studies have suggested that some substrates are likely to bind to OYEs in more

than one conformation, leading to low product enantiopurity.^[18] Indeed the moderate *ee* values obtained in some OYE-catalysed reductions of (*E*)-**1a** have been attributed to a combination of more than one binding orientation^[33] in addition to noncatalytic product racemisation under aqueous reaction conditions.^[7,8,18,34] It is possible that changes in the size and electronic properties of the side chains at positions 181 and 184 might perturb the binding geometry in such a way as to position the reducible C=C bond in a position suboptimal for hydride transfer from the FMN N5 atom compared to wild-type enzyme.^[22] As the majority of mutants (64%) showed an improvement in **1b** product enantiopurity, this suggests a shift in the ratio of substrate binding conformations compatible with alkene reduction in favour of (*S*)-**1b** formation. However, the often large increase in oxime formation is suggestive of an increase in the binding of the substrate in such a way as to position the nitro group optimal for overlap of the FMN N5 atom, effectively increasing the likelihood of nitro group reduction.

Comparative work on the reduction of a variety of α,β -unsaturated carbonyl compounds by OYEs in the presence of NAD(P)H and a number of cofactor recycling systems showed the source of reducing equivalents can sometimes impact significantly on the product yield, enantiopurity, switch the enantioselectivity and even affect the likelihood of generating side-products.^[1,8,9,17,34] Reactions of the mutants with (*E*)-**1a** in the presence of NADH often showed a significant increase in substrate conversion compared to the use of a NADP⁺/G6PDH recycling system (e.g., H184F; 24% vs 82%; Table 1). Surprisingly, in many cases the dramatic increases in substrate depletion were not accompanied by an increase in yields of (*S*)-**1b** product (typically <2%); this suggests that side-product formation was the dominant reaction (e.g., H181E/G/I and H184G/M/Y; Table S1 in the Supporting Information). Mutants H184N and H184R were seemingly unaffected by the source of reducing equivalents.

Mutant H184N is potentially useful because it showed only a moderate decrease in conversions, yields and oxime formation compared to wild type, yet showed a dramatic increase of *ee* from 42–54 to 85–87% (Table 1). Interestingly, asparagine is naturally found in this position in OYEs, such as OYE1^[21] and MR.^[15] Aerobic biotransformations of wild-type OYE1 with (*E*)-**1a** generated the *R* product with a range of enantiopurities (72–90% *ee*) depending on the source of the reducing equivalents.^[8] Therefore, the increase in enantiopurity of the (*S*)-**1b** product with H184N makes the enzyme more “OYE1-like”, except that the absolute configuration of the product differs. However, there was no mention of side-product/s formation with OYE1 and no yields were reported.^[8]

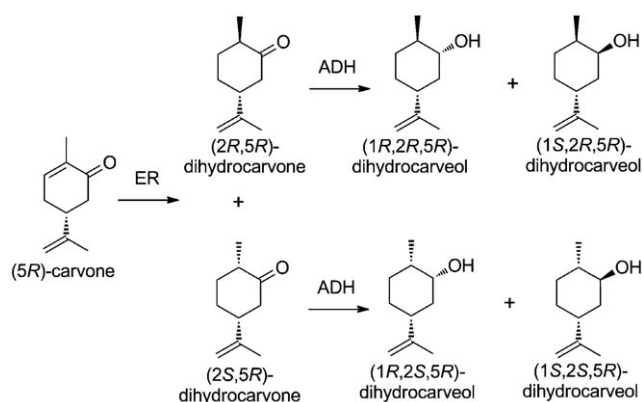
To further investigate this mutant we determined the anaerobic steady-state reaction parameters for PETN reductase H184N with NADPH and alkene **3a** (Table S2 and Figure S1 in the Supporting Information). The oxidation of NADPH by the H184N mutant showed a slight decrease in the apparent k_{cat} (2.5-fold) but has essentially the same K_{M} . This suggests that NADPH binding has not been compromised by the mutation, which is not surprising given that asparagine is present at this position in the majority of OYEs. This is in contrast to the re-

action with alkene **3a**, which results in an increase in both apparent K_{M} and apparent K_{i} (six- and ~fourfold, respectively). Mutant H184K is also useful since it generated (*S*)-**1b** with high enantiopurity (80–82% *ee*) and low oxime levels (3–7%). The almost threefold reduction in conversion/yields by H184K compared to wild-type enzyme can be compensated for by increasing the biocatalyst concentration.

Reduction of the terpenoid (5*R*)-carvone (**2a**) by wild-type enzyme is complete under our reaction conditions to produce the equivalent alkane product (2*R*,5*R*)-**2b** to good yields and high *de* (Table 1). An as yet unidentified side-product was also formed, which accounted for up to 25% of the product yield. All mutants were compromised to some degree in terms of the conversion and/or yields except for H184N, which retained essentially wild-type activity (Table 1 and Table S1 in the Supporting Information). The majority of the mutants showed conversions below 30%, and the product (2*R*,5*R*)-**2b** was obtained in moderate to good diastereoselectivity (typically >70% *de*). However, PETN reductase was more selective than a cell suspension of bryophytes (e.g., *Marchantia polymorpha*), which showed the formation of (2*R*,5*R*)-dihydrocarvone as well as a variety of side-products, such as (1*R*,2*R*,5*R*)-, (1*S*,2*R*,5*R*)-, (1*R*,2*S*,5*R*)- and (1*S*,2*S*,5*R*)-dihydrocarveol. These side-products were presumed to have formed due to the action of an alcohol dehydrogenase rather than being the inherent property of a constitutive enoate reductase(s) (Scheme 2).^[35]

Biotransformations of selected mutants against a variety of alkene substrates

A few mutants retaining significant activity against substrate (*E*)-**1a** were selected for further investigation to see if they showed improved biocatalytic activity against a variety of other activated α,β -unsaturated alkenes. The substrates screened were the classical OYE-like diketone substrates ketoisophorone (**4a**) and *N*-phenyl-2-methyl-maleimide (**5a**), the terpenoid citral **6a** and the aryl-nitropropenes (*E*)-**7a**–(*E*)-**9a** (Table 2 and Table S3 in the Supporting Information). Biotransformations with substrates **4a**–**6a** were performed with PETN



Scheme 2. Proposed mechanism of (5*R*)-**2a** reduction by bryophyte cell suspensions and identification of side-products; ER: enoate reductase(s); ADH: alcohol dehydrogenase(s); adapted from ref. [35].

reductase mutants H184N/Q/R/S/T under conditions that lead to both a complete conversion and high product enantiopurity with the wild-type enzyme. The short reaction time (1.5 h) for the substrate **4a** was applied to minimise water-mediated product racemisation that has been shown previously to significantly affect the product enantiopurity.^[17]

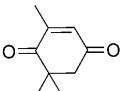
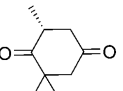
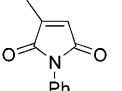
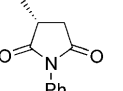
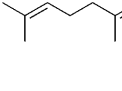
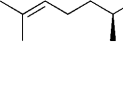
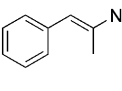
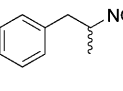
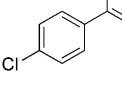
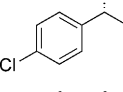
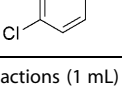
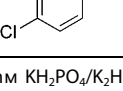
PETN reductase mutant, H184N, showed similar wild type conversions, yields and product enantiopurity with substrates **4a–7a** (Table 2). When differences were apparent, they were mostly confined to the conversion and yields as product enantiopurity and absolute configuration were little altered. Reactions of wild-type PETN reductase with alkene (*E*)-**7a** generated racemic products with minor side-product formation (Tables 2 and S3). All the mutants tested retained the high levels of substrate conversion, but unfortunately showed no improvements in product *ee*. However, the levels of the oxime by-product varied considerably, with mutant H181L showing an improvement over wild-type enzyme by having a slightly higher yield of product (*rac*)-**7b**. In all cases, the levels of oxime detected do not account fully for the loss in product yield; this suggests that other by-products were also formed. Based on reactions with (*E*)-**7a**, it is likely that the equivalent aldehyde and alcohol by-products were produced.

PETN reductase mutants all reduced 2-(4'-chloro-phenyl)-1-nitropropene ((*E*)-**8a**) with a dramatic increase in product enantiopurity, although with a decreased yield. This is similar to reactions with the related substrate (*E*)-**1a**, however, there was a significant improvement in the product yields (oxime levels not determined). Mutant H181N produced near optically pure (*S*)-**8b**, although at the expense of product yield. The lack of significant oxime formation in all reactions except wild type and H181N suggests that the low yield was due to the formation of other by-products or substrate/product decomposition compounds. This suggests that the presence of a *p*-chloro ring substituent in (*E*)-**8a** might prevent the substrate binding in a conformation compatible with nitro reduction in these mutants. In the case of the related substrate (*E*)-**9a**, neither H181N nor H184N showed significant improvements in conversion or product yields, and only H184N showed a similar reactivity to the wild type.

Oxime and aldehyde by-product formation

Reduction of the nitro-olefin (*E*)-**1a** by wild-type^[17,18] and mutant PETN reductases under anaerobic (Table 1) and aero-

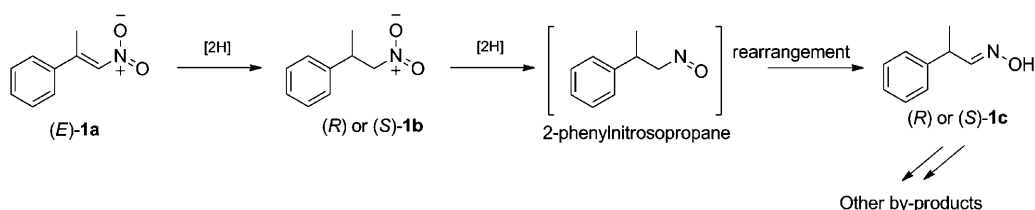
Table 2. Reduction of various activated alkenes by PETNR wild type and mutants by using NADP⁺/G6PDH cofactor regeneration system.^[a]

Substrate	Product	Enzyme	t [h]	Conv. ^[b] [%]	Yield ^[b] [%]	ee ^[c] [%]
4a 	<i>(R)</i> - 4b 	wild type	1.5	> 99	80	95
		H184N	1.5	> 99	83	96
		H184Q	1.5	63	54	94
		H184R	1.5	12	4	94
		H184S	1.5	> 99	90	95
		H184T	1.5	69	56	94
5a 	<i>(R)</i> - 5b 	wild type	1.5	> 99	> 99	> 99
		H184N	1.5	> 99	> 99	> 99
		H184Q	1.5	90	89	> 99
		H184R	1.5	90	88	87
		H184S	1.5	> 99	> 99	> 99
		H184T	1.5	98	96	> 99
6a 	<i>(S)</i> - 6b 	wild type	1.5	> 99	33	93
		H184N	1.5	> 99	35	95
		H184Q	1.5	31	8	94
		H184R	1.5	11	1	n.d.
		H184S	1.5	49	13	91
		H184T	1.5	16	3	82
<i>(E)</i> - 7a 	<i>(rac)</i> - 7b 	wild type	4	90	62 ^[d]	<i>rac</i>
		wild-type	48	> 99	93	<i>rac</i>
		H181N	48	91	80 ^[e]	<i>rac</i>
		H184N	48	> 99	92	<i>rac</i>
<i>(E)</i> - 8a 	<i>(S)</i> - 8b 	wild type	48	78	63 ^[e]	67
		H181N	48	70	19 ^[e]	98
		H184N	48	72	54	85
<i>(E)</i> - 9a 	<i>(R)</i> - 9b 	wild type	48	92	88	20
		H181N	48	36	30	8
		H184N	48	80	68	25

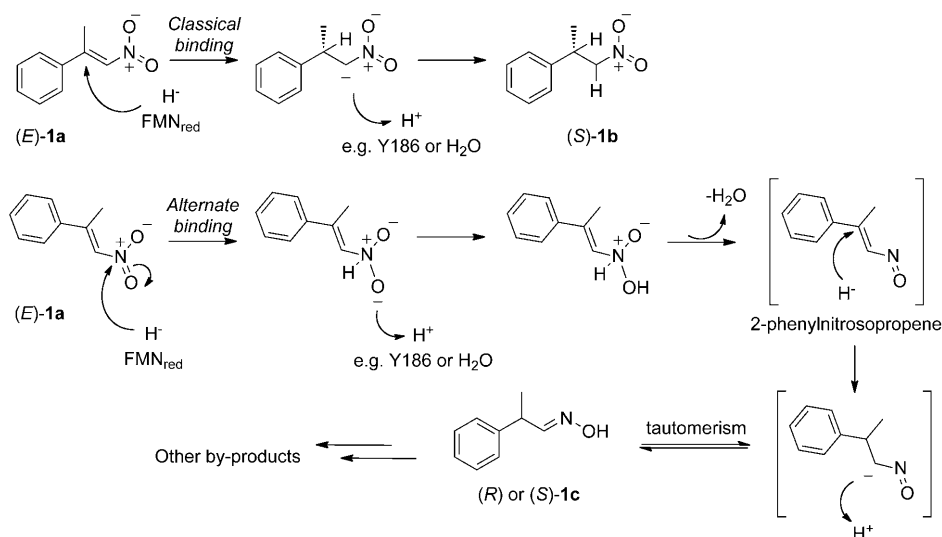
[a] Conditions: reactions (1 mL) were performed in buffer (50 mM KH₂PO₄/K₂HPO₄, pH 7.0), alkene (5 mM; added as a DMF solution with 2%, v/v, final concentration), PETNR (2 μM), glucose-6-phosphate dehydrogenase (8 U), glucose-6-phosphate (20 mM) and NADP⁺ (6 μM). Reaction mixtures were agitated at 30 °C and 130 rpm for 1.5–48 h. The results of the remaining mutants can be found in Table S3. [b] Yield of the equivalent alkane product determined by GC using a DB-Wax column; Conv.: % conversion is defined as the loss of substrate due to enzymatic reduction and noncatalytic decomposition; [c] Determined by either GC (DB-Wax column) or HPLC (Chiralcel OD column) as described in the Experimental Section. [d] No oxime formation was detected. [e] Significant oxime by-product detected. n.d.: not determined.

bic^[36] conditions resulted in the formation of significant quantities of by-products. To investigate this further, we ran a larger-scale biotransformation of (*E*)-**1a** with H181A and H184T mutants, which produced a significantly higher proportion of by-products. As with the wild-type reactions, the by-products 2-phenylpropanal oxime (**1c**), 2-phenylpropanal and 2-phenylpropanol were formed. There were also small quantities of 1-phenyl ethanol and 2-phenyl-3-nitropropene. We suggest that these latter products arise by hydration of the substrate. The resulting β -hydroxy nitroalkane can then undergo a nonenzymatic retro-Henry decomposition to yield acetophenone, followed by reduction to form 1-phenyl ethanol.^[36] Alternatively β -hydroxy nitroalkane could undergo β,γ -dehydration to 2-phenyl-3-nitropropene. Equivalent products phenylacetone oxime and phenylacetone were found in wild-type reactions with substrate (*E*)-**7a** (results not shown).

A recent report investigating the aerobic reduction of (*E*)-**1a** by the OYE enzymes PETN reductase, NerA, XenA-B, OPR3 (from *Lycopersicon esculentum*) and MR suggested that the formation of the oxime proceeds through a direct hydride transfer to the alkane product (*R*)- or (*S*)-**1b** to form the nitroso product.^[36] This was followed by spontaneous tautomerisation to form the oxime by-product (*R*)- or (*S*)-**1c** (Scheme 3). The authors proposed an additional OYE catalysed hydride transfer to the oxime would then form the unstable imine compound, which would hydrolyse spontaneously to form 2-phenylpropanal (*R*)- or (*S*)-**1d**. However, this report described this mechanism as proceeding by direct hydride delivery to the oxime nitrogen, which is not chemically viable. We propose that if biocatalytic oxime reduction were involved, hydride delivery must be at the oxime carbon, with O-protonation followed by dehydration to provide a route to yield the imine (cf. Scheme 4). The overall reduction of nitro compounds to produce carbonyl compounds was described as a biological equivalent of the Nef reaction.^[36] Interestingly, a similar route of nitrobenzene reduction to phenylhydroxylamine by the *Salmonella typhimuri-*



Scheme 3. Previously published mechanism of OYE-catalysed oxime (*E*)-**1c** formation by direct hydride transfer to the alkane (*E*)-**1b**; adapted from ref. [36].



Scheme 4. Proposed mechanism of alkane (*S*)-**1b** and oxime **1c** formation by wild-type and mutant PETN reductase-catalysed reduction of nitro-olefin, (*E*)-**1a**.

um nitroreductase, NRSa1, was proposed to proceed in a similar fashion.^[37]

Aerobic bioreductions of a variety of *rac* aliphatic nitroalkanes and their corresponding oximes by wild-type PETN reductase by others^[36] showed the formation of the equivalent aldehyde products, although at very low yields (2–10%). However, reactions to detect oxime ((*R*)- or (*S*)-**1c**) and aldehyde ((*R*)- or (*S*)-**1d**) formation from the alkane ((*R*)- or (*S*)-**1b**) were not reported. We carried out these reactions under our biotransformation conditions (anaerobic; 50 mM KH₂PO₄/K₂HPO₄, pH 7.0) with both wild-type and mutant PETN reductase, and 1–3 molar equivalents of NADH per substrate molecule. Surprisingly, reactions with alkane (*rac*)-**1b** yielded no detectable levels of oxime (*rac*)-**1c** and less than 1% of propionaldehyde **1d** (Table S4 in the Supporting Information). Significant loss of **1b** (12–31%) was detected, which is attributed to nitroalkane **1b** decomposition as seen previously (Table 1). Similar results were seen in reactions with the alkane (*rac*)-**7b**, although its decomposition was less prevalent. This is in contrast to a previous report showing 5–10% oxime formation in aerobic reactions of PETN reductase with (*rac*)-**1b**.^[36] Our reactions with oximes (*rac*)-**1c** and (*rac*)-**7c** showed <1% aldehyde formation and very little decomposition (1–4%). These results suggest that PETN reductase-catalysed oxime formation of **1c** under anaerobic conditions proceeds directly by reduction of the activated alkene (*E*)-**1a** rather than from the alkane **1b**.

We also looked at oxime and aldehyde formation by wild-type PETN reductase from alkene (*Z*)-**1a** and alkane product (*Z*)-**1b**. In this case, we carried out the reaction under aerobic conditions in two different buffers. The previous comparative studies with PETN reductase have shown that buffer conditions and/or the presence of oxygen can in some cases affect the product yield and enantiopurity.^[1,38] As expected,^[18] reduction of alkene (*Z*)-**1a** was fast and quantitative, and yielded product (*S*)-**1b** with high enantiopurity (Table S5 in the Supporting Information). No oxime **1c** was seen, and only trace levels of acetophenone were detected, most probably due to substrate decomposition. We did not observe any conversion of alkane (*rac*)-**1b** to the respective oxime or acetophenone formation under any buffer and oxygen level conditions.

We subjected three high oxime-producing H181X mutants (H181A/I/T) to a further high-resolution Ni-Sepharose purification step, which yielded near pure protein (>98%; results not shown) to ensure the presence of any contaminating *E. coli* enzymes was minimised. The reductions of alkenes (*E*)-**1a** and (*E*)-**7a** showed no significant differences in the yields of alkane, oxime and aldehyde products between the mutants of different purities (Table S6 in the Supporting Information). This suggests that contaminating *E. coli* enzymes are not likely to be responsible for oxime and/or aldehyde formation. In addition, the detection of minor side-products, such as the alcohol (*E*)-**1e** do not account for the differences between the conversions and yields. If the lack of detection of oxime/aldehyde/alcohol formation by PETN reductase reduction of (*rac*)-**1b** was due to degradation of these products by contaminating *E. coli* enzymes, then products (*E*)-**1c**, (*E*)-**1d** and (*E*)-**1e** should also be absent from reactions with alkene (*E*)-**1a**. As this was not the case, these results support the suggestion that PETN reductase wild-type-catalysed oxime **1c** formation proceeds through reduction of the activated alkene substrate rather than from the alkane product (Scheme 4). It is likely that PETN reductase requires the presence of a double bond next to the nitro group to enable nitro reduction to occur. This could be due to the conformational constraints of the planar alkene (*E*)-**1a** versus nonplanar alkane **1b**, which might permit a more favourable binding in a position compatible for nitro group reduction.

As such, we propose that nitro-olefins, such as (*E*)-**1a**, can bind in more than one conformation, with one complex positioning the nitro group within hydride transfer distance to the reduced FMN N5 atom. This might result in a direct hydride attack of the FMN on the substrate nitrogen atom followed by proton addition from water or an alternative proton donor (e.g., Y186; Scheme 4). Following the loss of a water molecule, the unstable 2-phenylnitrosopropene undergoes reduction to 2-phenylnitrosopropane, which tautomerises to form oxime **1c** (Scheme 4), followed by a further reaction to form the equivalent aldehyde and alcohol by-products. This could arise by oxime reduction and dehydration to the imine followed by hydrolysis (Scheme 4). Alternatively, a direct nonenzymatic oxime hydrolysis could occur. This pathway is similar to the abiotic reduction of a variety of nitrobenzene compounds to the corresponding anilines, by the equivalent nitrosobenzene and

phenylhydroxylamine, by mineral bound Fe^{II} as well as the nitroreductase activity of *Pseudomonas pseudoalcaligenes* JS45.^[39]

PETN reductase phenolic nitro-olefin binding and activity

Despite repeated attempts, no α - or β -alkyl- β -arylnitroalkene-bound OYE crystal structure has been determined due to the low substrate solubility, the predicted high K_d of complex formation and the potential for multiple substrate binding conformations.^[18] In an effort to overcome this problem, we synthesised a variety of hydroxy substituted 1-aryl-2-nitroethenes and 1-aryl-2-nitropropenes (*E*)-**10a**–(*E*)-**14a** (Figure S2 in the Supporting Information) with significantly improved solubilities. However, previous studies have shown that phenolic compounds, such as *p*-hydroxybenzaldehyde (**15a**; Figure S2 in the Supporting Information), inhibit oxidised OYEs, as the hydroxy group of the ligand interacts with the H181/H(N)184 couple.^[13,21,23] We studied the binding of ligands (*E*)-**10a** to (*E*)-**14a** with wild-type PETN reductase and determined both the activity and spectral changes upon binding of these compounds under aerobic conditions (Figure S2 in the Supporting Information).

Phenolic compounds perturb the FMN absorption spectrum by forming long wavelength absorbance bands around 500–800 nm upon inhibitor binding. A positive correlation between the energy of the long wavelength transition and the Hammett *para* constant suggests the formation of a charge-transfer complex (CTC) between the donor phenolate ion and the acceptor oxidised FMN isoalloxazine ring.^[24] As expected, characteristic long wavelength absorbance bands (550–650 nm) were seen in the interaction with phenolics (*E*)-**10a**–(*E*)-**11a** and (*E*)-**14a**–(*E*)-**15a** with PETN reductase; this is indicative of the formation of a CTC. However, a closer examination of the spectra showed that ligands (*E*)-**10a**–(*E*)-**11a** and (*E*)-**14a** had an unexpected increase in the peak at 464 nm, even after correction for the absorbance of the unbound compound spectra in this region (Figure S2 in the Supporting Information; purple lines). This suggests that the spectrum of the ligands had altered upon binding to enzyme, possibly by the formation of the equivalent anionic species, as suggested for the increase in absorbance at 320 nm upon phenol binding to oxidised OYE1.^[24] In the case of ligand (*E*)-**14a**, there is a known shift in the wavelength of the maximal absorbance peak from 363 to 456 nm after dissociation of the hydroxyl proton ($E_{363\text{ nm}} = 17800$ and $E_{456\text{ nm}} = 23200$, respectively).^[40] This change is more subtle with ligand (*E*)-**12a**, which displayed only a moderate change in the maximal absorbance wavelength after proton dissociation ($E_{318\text{ nm}} = 11300$ to $E_{331\text{ nm}} = 10200$, respectively).^[40]

The binding of 3-hydroxy substituted nitro-olefins (*E*)-**12a**–(*E*)-**13a** showed the characteristic decrease in absorbance of the FMN 464 nm peak, but to our surprise there was little to no evidence for formation of a CTC (Figure S2C–D in the Supporting Information). In general, a phenolate anion is required for formation of the CTC,^[24] however, a study of the binding of more than 30 phenolic compounds showed salicylic acid failed to produce a CTC band with OYE1, although it did bind to the enzyme and perturb the FMN spectrum.^[25] This was due to the

unusually high pK_a of 13.6 of the salicylic acid hydroxyl group compared to phenolics exhibiting CTC with OYE1, which had pK_a values ranging from 5.45 (pentafluorophenol) to 10.3 (*p*-cresol).^[25] However, the pK_a of (*E*)-**13a** is 9.08, so the absence of a CTC is not likely to be due to the absence of a phenolate ion.

We carried out biotransformation reactions with (*E*)-**10a**–(*E*)-**14a** to see if they could also bind in a productive conformation and undergo conventional C=C bond reduction. The five nonmethyl substituted compounds ((*E*)-**10a**, (*E*)-**12a** and (*E*)-**14a**) showed complete conversion, although poor alkane product yields were obtained with (*E*)-**12a** and (*E*)-**14a** (Table S7 in the Supporting Information). In contrast, lower conversions and racemic products were obtained from reactions with the methyl substituted (*E*)-**11a** and (*E*)-**13a**. The nonstoichiometric product yields for all reactions, except with (*E*)-**10a**, suggest significant substrate and/or product decomposition under the reaction conditions. Both the detection of charge-transfer complexes and alkene reduction suggest the presence of at least two binding conformations, with the H181/H184 couple likely binding to the nitro group and hydroxy group in active and inhibitory complexes, respectively. This supports previous activity and structural studies of PETN reductase that demonstrated or predicted multiple binding conformations with many substrates.^[17–19]

Crystal structures of substrate-bound wild-type and mutant PETN reductase

Given the remarkable changes in product enantiopurity and/or changes in the level of oxime formation with some mutants, we determined the crystal structures of two mutants H181N (1.2 Å) and H184N (2.2 Å) to see if the catalytic changes were due to major structural alterations within the active site (Figure S2 in the Supporting Information). In addition, structures of wild-type PETN reductase complexed with ligands (*E*)-**10a**, (*E*)-**12a** and (*E*)-**14a** were each determined to 1.2 Å (Figure 1) to see if one or more of the complexes had bound the substrate binding in a conformation compatible with alkene reduction. The data collection and refinement statistics of all five structures can be found in Table S8 in the Supporting Information.

All structures were found to be nearly identical to the wild-type PETN reductase structure (PDB ID: 1H50).^[27] Minor changes in specific active site residues (e.g., Y351, Q241) and the orientation of flexible loops (T273–P280 and N128–V143) were commonly seen in all structures. The FMN of each structure was modelled with a minor “butterfly-bend” in the isoalloxazine ring of the FMN prosthetic group, as seen in the “thermostable-like” OYE member TOYE^[16] and prior His₈-tagged structures.^[19] It is possible that this slight bending of the FMN in these PETN reductase structures is due to X-ray exposure during data collection. These structures show that the dramatic changes in product yields, enantiopurity and side-product formation of H181N and H184N are not due to major structural changes within the active site. Further detailed descriptions of the subtle changes in the active site of the mutant and co-crystal structures can be found in the Supporting Information

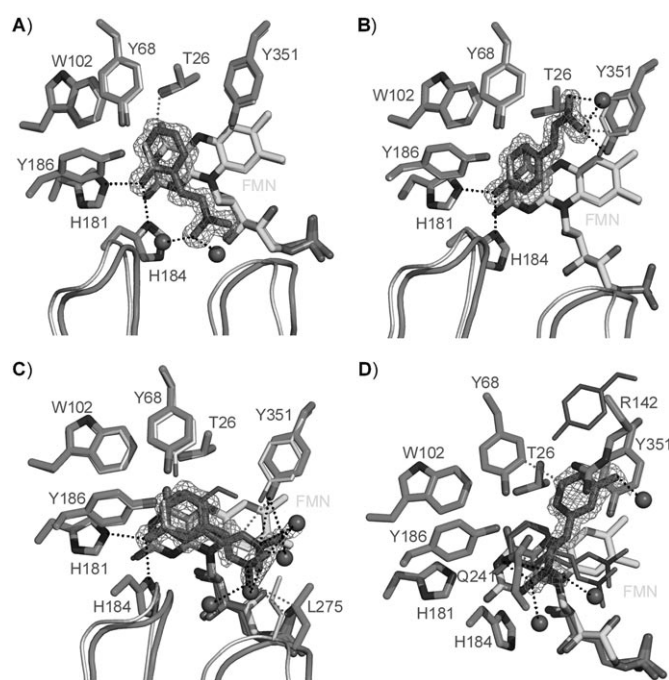


Figure 1. X-ray co-crystal structures of the active site of wild-type PETN reductase with bound inhibitors: A) (*E*)-**10a**, B) (*E*)-**14a**, and C) (*E*)-**12a**, superimposed with an acetate-bound wild-type enzyme structure (PDB ID: 1H50).^[27] The residues, FMN and inhibitors are shown as atom coloured sticks with green, yellow and magenta carbons, respectively. Acetate-bound structure residues are shown as atom coloured lines with grey carbons, while waters and interactions (clashes) are shown as red spheres and black (grey) dotted lines, respectively. Loops of the inhibitor- and acetate-bound structures T239–D244 (left) and T273–K279 (right) are shown as green cartoons and grey ribbons, respectively. The omit $|F_o| - |F_c|$ maps of the inhibitors are contoured at 1 σ (green mesh). D) X-ray co-crystal structure of the active site of the PETN reductase bound to (*E*)-**12a**, superimposed with the *p*-hydroxyaceto-phenone-bound structure of SYE1 (*Shewanella oneidensis* OYE1; PDB ID: 2GQ9).^[13] Three positions of (*E*)-**12a** are shown, with density present for the conformation not compatible with a charge-transfer complex. The residues and FMN are shown as atom coloured sticks with green and yellow carbons, respectively. Ligands (*E*)-**12a** and *p*-hydroxyacetophenone are shown as atom coloured lines (sticks for inhibitor within density) with magenta and blue carbons, while waters and interactions (clashes) are shown as red spheres and black (grey) dotted lines, respectively. The omit $|F_o| - |F_c|$ map of the inhibitor is contoured at 1 σ (green mesh). All figures were generated in PyMOL.^[41]

(Figure S3 and associated discussion in the Supporting Information).

The omit map $|F_o| - |F_c|$ of the (*E*)-**10a**-bound wild-type PETN reductase structure shows clear density for a single position of the ligand (Figure 1A). Given the observed charge-transfer complex spectra of PETN reductase in the presence of (*E*)-**10a**, it was not surprising that the co-crystal structure showed the ligand binding in an inhibitory complex with the 2'-hydroxy atom O2' forming hydrogen bonds with both H181 NE2 and H184 ND1 atoms (Table S9 in the Supporting Information). This is consistent with the co-crystal structures of PHB-bound YqjM^[23] and SYE1 (OYE from *Shewanella oneidensis*),^[13] which showed the phenolic oxygen interacting with the H181 and H/N184 residue pair. This is not surprising as the presence of positively charged groups, such as residues H181/H(N)184, might be required to stabilise the phenolate anion.^[24]

The aromatic ring is positioned partially above the *si* face of the FMN isoalloxazine ring (C4'–N5 separation distance of 3.5 Å), with the planes of the two rings nearly parallel, as seen in the *p*-hydroxybenzaldehyde (PHB)-bound OYE1 structure.^[21] It has been proposed that planar stacking of the inhibitor aromatic group and FMN isoalloxazine ring might maximise the interaction between their π electrons.^[42] The alkyl nitroalkene group is located close to, but does not interact with the side chain of H184. There is a change in the orientation of flexible loops between residues T273–P280 and N128–V143, presumably to accommodate the binding of the inhibitor. In addition, there was a shift in position of the side chains of residues T26 and Y351. A minor clash was seen between the aromatic ring atom C4' of (*E*)-**10a** and residue T26 OG1; this could explain the minor change in position of this residue compared to the wild-type structure.

Interestingly, alignment of the three inhibitor-bound structures with wild-type acetate-bound PETN reductase showed that the inhibitor atoms O2', C2', C3' and C1' ((*E*)-**10a** numbering) bind in very similar positions to acetate atoms OXT, C, CH3 and O, respectively (Figure 1A). There were two additional hydrogen bonds present, however, they were between atom O2 of the nitro group and two water molecules.

The omit map electron density map $|F_o| - |F_c|$ of the (*E*)-**14a**-bound PETN reductase structure showed clear density for a single position of the ligand (Figure 1B). Similar to the (*E*)-**10a**-bound structure, the phenolic oxygen O4' interacts with both H181 NE2 and H184 ND1 atoms. As a consequence of this, the alkyl nitroalkene group points towards the surface of the protein, with the nitro group located between the terminal OG atoms of residues Y68 and Y351. In this position, inhibitor atom O1 forms a hydrogen bond with Y351 OH. However, there were also clashes between the O1 and N atoms and Y351 C2 and CE1, respectively (Table S9 in the Supporting Information). To minimise the clashes between the nitro group and Y351, the aromatic ring is not parallel to the FMN isoalloxazine ring (C2'–N5 separation distance of 3.7 Å), with a deviation angle of approximately 15°. Both the O1 and O2 atoms form a hydrogen bond with a water molecule.

Surprisingly, the omit electron density map $|F_o| - |F_c|$ of the (*E*)-**12a**-bound PETN reductase structure showed density for two nonoverlapping binding sites of the inhibitor (Figure 1C–D). At one binding site, the phenolic group is positioned in a similar orientation as the (*E*)-**10a**-bound structure (C5'–N5 separation distance of about 3.4 Å). However, the density for the nitroalkene component of the inhibitor is more diffuse, which suggests that two conformations are present (402A/B). The second molecule (402B) has been modelled based on a similar position of the phenolic group with the nitroalkane functionality rotated about the C1'–C2 bond (Figure 1C). The two positions of the nitroalkene group are located slightly below the plane of the phenolic ring, with the nitro group positioned close to residue L275. In both conformations, the O3' atom of the inhibitor interacts with both H181 NE2 and H184 ND1 (Table S9 in the Supporting Information). Additional interactions between the inhibitor 402A and PETN reductase are de-

scribed in Table S9 and the accompanying discussion in the Supporting Information.

The second binding mode of the inhibitor (*E*)-**12a** (403) is located in front of the 402A/B position, rotated about 45°, which positions the phenolic group above the plane of the FMN isoalloxazine ring and between residues R142 and Y351 (C2'–N5 separation distance of 6.5 Å; Figure 1D). The phenolic O3' and nitro group O1 and O2 atoms are hydrogen bonded to water molecules, while both the O1 and N1 atoms interact with Q241 NE2 (Table S9 in the Supporting Information). In this position, a charge-transfer complex between the inhibitor and FMN is not possible. The electron density for this binding site showed that it was not fully occupied. This suggests that there was a second conformation of the inhibitor at this binding site, with the nitroalkene group rotated as in molecule 402B. However, due to the low occupancy of this position, it has not been modelled into the structure.

The binding of the alkene (*E*)-**12a** in the classical charge-transfer complex orientation (phenolic OH binding to H181/184) is surprising given the near absence of a charge-transfer complex between PETN reductase, and the ability of PETN reductase to catalyse conventional alkene reduction with this substrate. However, the multiple ligand binding modes seen structurally suggest that the apparent lack of a charge-transfer complex might be due to the overall low occupancy of this species. This could be an example of a protein–ligand complex with possibly multiple conformational states, with the thermodynamically more metastable state “frozen-out” in the crystal structure. This could also explain the crystal structures showing the ligands binding in the inhibitory, rather than the catalytically active conformation(s).

We also determined the co-crystal structures of wild-type PETN reductase and the α -methyl substituted ligands (*E*)-**11a** (2.1 Å) and (*E*)-**13a** (1.6 Å); however, they showed only partial density for the ligands bound in virtually identical positions to their respective nonmethylated counterpart structures (results not shown). An additional co-crystal structure was determined between PETN reductase and (*E*)-1-(4'-phosphophenyl)-2-nitroethene; this showed the phosphate group coordinating with H181 and H184 (unpublished results). We also attempted to determine the more soluble methoxy substituted nitro-olefin-bound PETN reductase structures, however, crystallisation trials were unsuccessful (results not shown). Therefore, there are presently no crystal structures of the binding mode(s) of nitro-olefins (*E*)-**1a** and (*E*)-**7a–9a** to any OYE in an active conformation consistent with alkene and/or nitro group reduction. However, modelling studies and the known product stereochemistry enables us to predict likely conformation(s) compatible for alkene and/or nitro group reduction.^[17]

Conclusions

PETN reductase and other OYEs are catalytically promiscuous as significant quantities of the equivalent oxime and aldehyde side-products are formed alongside the nitroalkane during the reduction of the nitroalkene (*E*)-**1a**. This shows the ability to catalyse both alkene and nitro group reduction within the

same substrate. Mutagenesis of a key substrate-binding residue H181 was remarkably successful in enhancing the yield of the oxime product(s). This demonstrates that it is possible to profoundly alter the catalytic selectivity of the enzyme by a single residue change. In some cases, single site mutations resulted in the almost total abolition of native alkane product (S)-**1b** formation. Similar mutations at a second key substrate-binding residue H184 had more moderate effects on the levels of oxime formation, with a higher retention of alkene reduction and significantly higher product enantiopurities. The majority of the mutants retained activity demonstrating the plasticity and adaptability of the substrate binding site in allowing substrate binding to occur in the majority of the mutants. However, the often high levels of oxime formation suggest an alteration in the position and orientation of the substrate binding. Mutations at residues H181 and H184 likely alter the substrate binding site in a manner that prevents optimal positioning of the substrate C=C bond relative to the FMN N5 atom. In addition, changing the nature of residue(s) close to the flavin isoalloxazine ring might influence electronic properties of the flavin, such as the redox potential. As these residues are thought to be involved in increasing the electronegativity of the substrate activating group, mutations that enhance or decrease this ability could also effect the catalytic rate. However, detailed kinetic and potentiometric studies of each mutant are required to determine this, which is beyond the scope of this study.

Oximes are useful industrially in a broad range of applications, such as antioxidants in paints, tape adhesives, precursors for agricultural pesticides^[43] and more recently a potential role in human immunodeficiency virus (HIV-1) protease-inhibiting pharmaceuticals.^[44] Biocatalytic oxime formation has been reported previously, such as the formation of aldoxime by the actinomycete *Nocardia uniformis* subsp. *tsuyamanensis* (cytochrome P450 NoCL) in the biosynthesis of the monocyclic β -lactam antibiotic nocardicin A.^[45] Given the success in converting an "ene"-reductase into primarily a nitroreductase by a single amino acid change, further mutagenesis might improve the oxime formation capability of PETN reductase, by screening against more industrially relevant compounds. One potential target is the reduction of 1-nitrocyclohexene into the equivalent oxime, which in the presence of sulfuric acid undergoes the Beckmann rearrangement to form caprolactam, a precursor in Nylon 6 synthesis.^[46] At present, no wild-type PETN reductase oxime formation from 1-nitrocyclohexene has been detected,^[18] however, one report suggests a possibility of a low level of oxime formation from nitrocyclohexane (5%).^[36] Therefore, PETN reductase mutants could be a promising target for the biocatalytic formation of synthetically useful oximes.

The importance of the nature of the electronegative group in activated alkene reduction was highlighted by the preference of residues H181 and H184 to bind to the phenolic rather than the nitro group in hydroxyphenyl substituted nitroethenes and nitropropenes (*E*)-**10a**–(*E*)-**14a**. Studies that attempt to expand the substrate range of OYEs need to consider the potential of the formation of multiple binding modes, some of which might be inactive states, when more than one electro-

negative group is present in the substrate. In addition, the absence of a characteristic charge-transfer complex spectral signal does not necessarily indicate the absence of an inhibitory complex, but could suggest the possibility of multiple ligand binding states.

The use of high-resolution structural information and/or modelling of both wild-type and mutated enzymes has proven useful to analyse the role of individual residues in substrate binding and/or catalysis. The relatively minor structural changes seen in both the H181N, H184N and inhibitor-bound structures compared to wild-type enzyme shows that wide-ranging global changes in enzyme structure might not be always necessary to cause significant changes in catalytic selectivity. Subtler, more localised changes resulted in more significant backbone shifts of flexible active site loops. These were sufficient to compensate for both specific amino acid residue changes and ligand binding. These features combined with the catalytic promiscuity and relative large active site of OYEs make them important targets for further mutagenesis studies to generate more useful biocatalysts.

Experimental Section

General: All reagents were of analytical grade. All biotransformation reactions were set up within an anaerobic glove box (Belle Technology, Ltd.) under a nitrogen atmosphere (<5 ppm oxygen). The concentration of PETN reductase and substrates were determined by the extinction coefficients method by using values described previously.^[17,18,33] All medium components were obtained from Formedium.

Identification of H181X and H184X mutants: Single site-saturated libraries of PETN reductase-His₆ at positions H181 and H184 (96 clones per library) were generated by PCR with NNK degenerate oligonucleotides, followed by automated robotic colony picking, culture growth of 96 clones per mutation position and glycerol stock formation.^[19] Library members were selected at random and sequenced to identify each of the possible 19 mutants at positions H181 and H184, with 80 and 64% of each library screened, respectively. Each mutant was maintained as a frozen glycerol stock of the *E. coli* strain JM109. The stocks were used to inoculate 5 mL of Luria Broth (LB; 5 g L⁻¹ yeast extract, 10 g L⁻¹ tryptone, 10 g L⁻¹ NaCl) containing ampicillin (100 μ g mL⁻¹) and grown for 24 h at 37 °C. The plasmid containing the mutated PETN reductase gene (pONR1)^[47] was extracted and purified from each clone by using the QIAprep spin miniprep kit (Qiagen), according to the manufacturer's protocol. Full gene sequences of all mutants were confirmed by DNA sequencing (Eurofins MWG Operon). Only 13 of the possible 19 H181X mutants were identified (H181A, H181C, H181D, H181F, H181I, H181L, H181N, H181Q, H181R, H181S, H181T, H181V, and H181Y) while all H184X mutants, except H184Q, were found.

Site-directed mutagenesis: The remaining mutants were generated by site-directed mutagenesis by using the Stratagene Quick-Change whole plasmid synthesis protocol. PCR reactions were performed by using the PETN reductase-His₆ modified template. Details of the respective oligonucleotides used in each PCR can be found in the Supporting Information document. Despite repeated attempts, no PCR product was obtained for the H184Q mutant, so further work was abandoned. Following template removal by selective restriction digest (DpnI), PCR products (50 ng) were transformed into the *E. coli* strain JM109 (Promega) according to the

manufacturer's protocol. Each mutant was grown on LB agar containing ampicillin ($100 \mu\text{g mL}^{-1}$) for 24 h at 37°C . Colonies (2–5) of each mutant were grown and fully sequenced, as above, to confirm the presence of the required mutations. The following mutants were obtained by using this process: H181E, H181G, H181K, H181M, H181P and H181W.

Enzyme production and purification: Wild-type non-His₈-tagged PETN reductase was prepared as described previously.^[27] PETN reductase-His₈ wild-type and mutant cultures (3 L) were grown in Terrific broth autoinduction medium (TBAlM) containing ampicillin ($100 \mu\text{g mL}^{-1}$) for 24 h at 37°C . Cells were harvested by centrifugation at $6000g$ for 30 min at 5°C (Avanti J-26 XP; Beckman Coulter). Cell pellets were resuspended in lysis buffer (50 mM $\text{KH}_2\text{PO}_4/\text{K}_2\text{HPO}_4$ pH 7.0 containing the Roche EDTA-free complete protease inhibitor cocktail, 0.1 mg mL^{-1} DNase I, 1 mg mL^{-1} lysozyme and excess free FMN) and disrupted by the addition of 1×Bugbuster (Novagen). The slurry was gently agitated for 10 min at room temperature followed by extract clarification by centrifugation for 30 min at $26600g$. The supernatant was dialysed into 50 mM $\text{KH}_2\text{PO}_4/\text{K}_2\text{HPO}_4$ pH 7.0 (5 L) to remove the detergent followed by the addition of imidazole (10 mM) and NaCl (300 mM).

PETN reductase-His₈ wild-type and mutant enzymes were purified by binding the extracts to a Ni-IDA column (10 mL; Generson), pre-equilibrated in buffer A (50 mM $\text{KH}_2\text{PO}_4/\text{K}_2\text{HPO}_4$ pH 7.0 containing 0.3 M NaCl, 10 mM imidazole). The column was washed with 3–5× column volumes of buffer B (50 mM $\text{KH}_2\text{PO}_4/\text{K}_2\text{HPO}_4$ pH 7.0 containing 0.3 M NaCl, 20 mM imidazole) followed by elution with a step to buffer C (50 mM $\text{KH}_2\text{PO}_4/\text{K}_2\text{HPO}_4$ pH 7.0 containing 0.3 M NaCl, 250 mM imidazole). Purity was assessed by SDS-PAGE (>90%) and the concentration of active enzyme was determined by using the extinction coefficient method.^[17,18]

Spectroscopic techniques: All spectra were determined aerobically by using a Cary UV-50 Bio UV/vis scanning spectrophotometer in a 1 mL quartz cuvette (Hellma) with a 1 cm path-length. The absorbance spectrum of each purified PETN reductase wild type, H181X and H184X mutants (4–66 μM) were determined between 200–800 nm. Spectra were normalised at 325 nm for ease of comparison with the wild-type enzyme. The inhibitor-bound enzyme complexes (1 mL) were formed by combining wild-type PETN reductase (30 μM) with (E)-10a to (E)-15a in buffer (50 mM $\text{KH}_2\text{PO}_4/\text{K}_2\text{HPO}_4$ pH 7.0) at room temperature. The absorbance spectra were taken between 200 and 800 nm and compared to both free enzyme and free inhibitor. Due to the significant overlap between the spectra of the inhibitors and NADPH, no steady state kinetic assays were performed.

Steady-state kinetic analysis: PETN reductase H184N was deoxygenated by passage through a BioRad 10DG column equilibrated in anaerobic reaction buffer (50 mM $\text{KH}_2\text{PO}_4/\text{K}_2\text{HPO}_4$ pH 7). Steady state analyses were performed on a Cary UV-50 Bio UV/Vis scanning spectrophotometer by using a 1 mL quartz cuvette (Hellma) with a 1 cm path-length. Reactions (1 mL) were performed in $\text{KH}_2\text{PO}_4/\text{K}_2\text{HPO}_4$ (50 mM, pH 7) containing NADPH (0–0.25 mM), PETN reductase (0–5 μM) and alkene 3a (0–50 mM, added as concentrated stocks in ethanol (final reaction concentration of 5%, v/v)). All reactions were followed continuously by monitoring NADPH oxidation at 340 nm for 1 min at 25°C . The concentration of enzyme, NADPH and alkene 3a were determined by the extinction coefficient method by using values determined previously.^[17]

Biotransformations with PETN reductase: Details of ligand synthesis and biotransformation analytical procedures are described in the Supporting Information document. PETN reductase wild type

and mutants were deoxygenated into anaerobic reaction buffer as described above. The concentration of enzyme, NAD(P)H and substrates within the reactions were determined by the extinction coefficient method by using values determined previously.^[17] Standard reactions for the mutants (1.0 mL) were performed in buffer (50 mM $\text{KH}_2\text{PO}_4/\text{K}_2\text{HPO}_4$ pH 7.0) containing alkene (5 mM; added as a DMF solution with 2%, v/v, final concentration), NADH (6–15 mM) and PETN reductase (2 μM). The reactions were shaken at 37°C at 130 rpm for 1.5–48 h followed by reaction termination by extraction with ethyl acetate (0.9 mL) containing an internal standard, and dried by using MgSO_4 . The extracts were analyzed by GC or HPLC to determine the %yield (amount of alkane/oxime/aldehyde product formed), %conversion (substrate consumption), and enantiomeric excess as described previously.^[17,18,33] When significant side-products were detected, further reactions were carried out in larger scale (5 mL) by using the reaction conditions above and the individual side-products were extracted and purified by flash chromatography (hexane/ethyl acetate, 4:1).

In some cases, wild-type and mutant enzyme biotransformations were carried by using a NADP⁺/glucose-6-phosphate dehydrogenase cofactor regeneration system in the place of NAD(P)H.^[17,18] Reactions with the hydroxy substituted 1-phenyl-2-nitroethenes and 1-phenyl-2-propenes with wild-type enzyme were performed as described for the standard reaction with NADH for 24 h at 30°C . To determine if wild-type PETN reductase can reduce the nitroalkanes (R/S)-1b, (R/S)-7b and oxime side products (R/S)-1c and (R/S)-7c, standard reactions were performed as above, by substituting the alkene for the respective product, in the presence of NAD(P)H (5–15 mM) for 6 h at 30°C and 130 rpm. In addition, reactions were performed with product (rac)-1b in the presence of NAD(P)H (6 mM), wild-type PETN reductase (2 mM), in either phosphate (50 mM $\text{KH}_2\text{PO}_4/\text{K}_2\text{HPO}_4$ pH 7.0) or Tris buffer (50 mM, pH 7.5) under aerobic conditions at 30°C for 45 h at 130 rpm. Conversion rates were compared to reactions with the equivalent alkene substrates (E)-1a and (E)-7a, and control reactions were performed in the absence of cofactor.

Crystallogensis and data collection: Crystals of oxidised PETN reductase wild type and His₈-tagged H181N and H184N mutants were grown by using the sitting-drop method in buffer D (100 mM sodium cacodylate, pH 6.2, containing 100 mM sodium acetate, 16–18% isopropanol, 18–22% polyethylene glycol 3000) for 3 days at 20°C . Wild-type crystals were back-soaked in buffer E (100 mM sodium cacodylate, pH 6.2, containing 16–18% isopropanol, 18–22% poly(ethylene glycol) 3000) for about 5 min at room temperature to remove the acetate bound to the active site of the enzyme. A second soak was performed in buffer E containing saturating levels of the inhibitors (E)-10a, (E)-12a or (E)-14a for 30 s to 5 min at room temperature. All crystals were flash frozen in liquid nitrogen in the absence of additional cryoprotectant.

Full PETN reductase-His₈ H181N mutant (1.2 Å) and native PETN reductase (E)-10a-bound (1.2 Å) X-ray diffraction data sets were collected from single crystals at the European Synchrotron Radiation Facility (Grenoble, France) on Station ID 14.4 (wavelength 1.07 Å; 100 K) by using an ADSC CCD detector. A full H184N PETN reductase-His₈ (2.2 Å) X-ray diffraction data set was collected in-house from a single crystal by using a Bruker Microstar generator (wavelength 1.542 Å; 100 K) with an X8 Proteum CCD detector. Full (E)-12a- (1.2 Å) and (E)-14a-bound (1.2 Å) native PETN reductase X-ray diffraction data sets were collected from single crystals at the Diamond Light Source (Oxford, UK) on beamline IO2 (wavelength 0.979 Å; 100 K) by using an ADSC Q315 CCD detector.

Structure determination and refinement: The PETN reductase-His₈ H184N data set was processed by using the Proteum2/SAINT software.^[48] All remaining data sets were processed and scaled by using MOSFLM^[49] and Scala.^[50] The structures were solved by molecular replacement by using the coordinates for the acetate-bound PETN reductase structure (PDB ID: 1H50).^[27] Model rebuilding and water addition was performed automatically by using REFMAC combined with ARP/warp.^[51] Positional and anisotropic (isotropic for H184N) B-factor refinement was performed by using REFMAC5^[52] (hydrogen atoms included in the refinement except for H184N), with alternate rounds of manual rebuilding of the model in COOT.^[41]

The final models were refined to 1.20, 2.20, 1.20, 1.20 and 1.2 Å resolution to give final $R_{\text{factor}}/R_{\text{free}}$ of 13.6/15.9, 14.8/22.1, 12.5/14.7, 13.2/15.5 and 12.1/14.0 for PETN reductase-His₈ mutants H181N, H184N and the (E)-10a-, (E)-12a- and (E)-14a-bound native PETN reductase structures, respectively. The atomic coordinates and structure factors (PDB ID codes: 3P74, 3P82, 3P7Y, 3P80 and 3P81, respectively) have been deposited in the Protein Data Bank, Research Collaboratory for Structural Bioinformatics, Rutgers University, New Brunswick, NJ (<http://www.rcsb.org/>).

Acknowledgements

This work was funded by UK Biotechnology and Biological Sciences Research Council (BBSRC). N.S.S. is a BBSRC Professorial Research Fellow and a Royal Society Wolfson Merit Award holder.

Keywords: asymmetric bioreduction • biocatalysis • PETN reductase • unsaturated alkenes • X-ray crystallography

- [1] H. S. Toogood, J. M. Gardiner, N. S. Scrutton, *ChemCatChem* **2010**, *2*, 892–914.
- [2] N. J. Turner, *Trends Biotechnol.* **2003**, *21*, 474–478.
- [3] *Catalytic Asymmetric Synthesis*, 3rd ed. (Ed.: I. Ojima), Wiley, Hoboken, **2010**.
- [4] R. R. Chirumamilla, R. Muralidhar, R. Marchant, P. Nigam, *Mol. Cell. Biochem.* **2001**, *224*, 159–168; S. Panke, M. Held, M. Wubbolds, *Curr. Opin. Biotechnol.* **2004**, *15*, 272–279; M. T. Reetz, D. Kahakeaw, J. Sanchis, *Mol. Biosyst.* **2009**, *5*, 115–122.
- [5] S. Luetz, L. Giver, J. Lalonde, *Biotechnol. Bioeng.* **2008**, *101*, 647–653.
- [6] J. F. Chaparro-Riggers, T. A. Rogers, E. Vazquez-Figueroa, K. M. Polizzi, A. S. Bommarius, *Adv. Synth. Catal.* **2007**, *349*, 1521–1531; C. Stueckler, M. Hall, H. Ehammer, E. Pointner, W. Kroutil, P. Macheroux, K. Faber, *Org. Lett.* **2007**, *9*, 5409–5411; M. A. Swiderska, J. D. Stewart, *Org. Lett.* **2006**, *8*, 6131–6133; M. A. Swiderska, J. D. Stewart, *J. Mol. Catal. B* **2006**, *42*, 52–54.
- [7] M. Hall, C. Stueckler, H. Ehammer, E. Pointner, G. Oberdorfer, K. Gruber, B. Hauer, R. Stuermer, W. Kroutil, P. Macheroux, K. Faber, *Adv. Synth. Catal.* **2008**, *350*, 411–418.
- [8] M. Hall, C. Stueckler, B. Hauer, R. Stuermer, T. Friedrich, M. Breuer, W. Kroutil, K. Faber, *Eur. J. Org. Chem.* **2008**, 1511–1516.
- [9] M. Hall, C. Stueckler, B. Hauer, R. Stuermer, W. Kroutil, P. Macheroux, K. Faber, *Biotrans—8th International Symposium on Biocatalysis and Bio-transformations*, Oviedo, Spain, **2007**.
- [10] O. Warburg, W. Christian, *Naturwissenschaften* **1932**, *20*, 688.
- [11] P. R. Binks, C. E. French, S. Nicklin, N. C. Bruce, *Appl. Environ. Microbiol.* **1996**, *62*, 1214–1219.
- [12] T. B. Fitzpatrick, N. Amrhein, P. Macheroux, *J. Biol. Chem.* **2003**, *278*, 19891–19897.
- [13] D. van den Hemel, A. Brige, S. N. Savvides, J. Van Beeumen, *J. Biol. Chem.* **2006**, *281*, 28152–28161.
- [14] F. Schaller, E. W. Weiler, *J. Biol. Chem.* **1997**, *272*, 28066–28072.
- [15] C. E. French, N. C. Bruce, *Biochem. J.* **1995**, *312*, 671–678.
- [16] B. V. Adalbjörnsson, H. S. Toogood, A. Fryszkowska, C. R. Pudney, T. A. Jowitt, D. Leys, N. S. Scrutton, *ChemBioChem* **2010**, *11*, 197–207.
- [17] A. Fryszkowska, H. S. Toogood, M. Sakuma, J. M. Gardiner, G. M. Stephens, N. S. Scrutton, *Adv. Synth. Catal.* **2009**, *351*, 2976–2990.
- [18] H. S. Toogood, A. Fryszkowska, V. Hare, K. Fisher, A. Roujeinikova, D. Leys, J. M. Gardiner, G. M. Stephens, N. S. Scrutton, *Adv. Synth. Catal.* **2008**, *350*, 2789–2803.
- [19] M. E. Hulley, H. S. Toogood, A. Fryszkowska, D. Mansell, G. M. Stephens, J. M. Gardiner, N. S. Scrutton, *ChemBioChem* **2010**, *11*, 2433–2447.
- [20] B. J. Brown, Z. E. Deng, P. A. Karplus, V. Massey, *J. Biol. Chem.* **1998**, *273*, 32753–32762.
- [21] K. M. Fox, P. A. Karplus, *Structure* **1994**, *2*, 1089–1105.
- [22] H. Khan, T. Barna, N. C. Bruce, A. W. Munro, D. Leys, N. S. Scrutton, *FEBS J.* **2005**, *272*, 4660–4671.
- [23] K. Kitzing, T. B. Fitzpatrick, C. Wilken, J. Sawa, G. P. Bourenkov, P. Macheroux, T. Clausen, *J. Biol. Chem.* **2005**, *280*, 27904–27913.
- [24] A. S. Abramovitz, V. Massey, *J. Biol. Chem.* **1976**, *251*, 5327–5336.
- [25] A. S. Abramovitz, V. Massey, *J. Biol. Chem.* **1976**, *251*, 5321–5326.
- [26] T. Barna, H. L. Messiha, C. Petosa, N. C. Bruce, N. S. Scrutton, P. C. Moody, *J. Biol. Chem.* **2002**, *277*, 30976–30983.
- [27] T. M. Barna, H. Khan, N. C. Bruce, I. Barsukov, N. S. Scrutton, P. C. Moody, *J. Mol. Biol.* **2001**, *310*, 433–447.
- [28] H. Khan, R. J. Harris, T. Barna, D. H. Craig, N. C. Bruce, A. W. Munro, P. C. Moody, N. S. Scrutton, *J. Biol. Chem.* **2002**, *277*, 21906–21912.
- [29] D. J. Bougioukou, S. Kille, A. Taglieber, M. T. Reetz, *Adv. Synth. Catal.* **2009**, *351*, 3287–3305.
- [30] C. Jäckel, P. Kast, D. Hilvert, *Annu. Rev. Biophys.* **2008**, *37*, 153–173.
- [31] U. T. Bornscheuer, R. J. Kazlauskas, *Angew. Chem.* **2004**, *116*, 6156–6165; *Angew. Chem. Int. Ed.* **2004**, *43*, 6032–6040.
- [32] Y. Yoshikuni, T. E. Ferrin, J. D. Keasling, *Nature* **2006**, *440*, 1078–1082.
- [33] A. Fryszkowska, K. Fisher, J. M. Gardiner, G. M. Stephens, *J. Org. Chem.* **2008**, *73*, 4295–4298.
- [34] M. Hall, C. Stueckler, W. Kroutil, P. Macheroux, K. Faber, *Angew. Chem.* **2007**, *119*, 4008–4011; *Angew. Chem. Int. Ed.* **2007**, *46*, 3934–3937.
- [35] A. Speicher, A. Roeser, R. Heisel, *J. Mol. Catal. B* **2003**, *22*, 71–77.
- [36] K. Durchschein, B. Ferreira-da Silva, S. Wallner, P. Macheroux, W. Kroutil, S. M. Glueck, K. Faber, *Green Chem.* **2010**, *12*, 616–619.
- [37] Y. Yanto, M. Hall, A. S. Bommarius, *Org. Biomol. Chem.* **2010**, *8*, 1826–1832.
- [38] N. J. Mueller, C. Stueckler, B. Hauer, N. Baudendistel, H. Housden, N. C. Bruce, K. Faber, *Adv. Synth. Catal.* **2010**, *352*, 387–394.
- [39] T. B. Hofstetter, J. C. Spain, S. F. Nishino, J. Bolotin, R. P. Schwarzenbach, *Environ. Sci. Technol.* **2008**, *42*, 4764–4770.
- [40] R. Stewart, L. G. Walker, *Canadian J. Chem.* **1957**, *35*, 1561–1569.
- [41] W. L. DeLano, *The PyMOL User's Manual*, DeLano Scientific, Palo Alto, CA, USA, **2002**.
- [42] R. Foster, *Organic Charge-Transfer Complexes*, Academic Press, New York, **1969**, 42–56.
- [43] N. G. Love, R. J. Smith, K. R. Gilmore, C. W. Randall, *Water Environ. Res.* **1999**, *71*, 418–425.
- [44] T. Komai, R. Yagi, H. Suzuki-Sunagawa, Y. Ishikawa, A. Kasuya, S. Miyamoto, H. Handa, *Biochem. Biophys. Res. Commun.* **1997**, *230*, 557–561.
- [45] W. L. Kelly, C. A. Townsend, *J. Am. Chem. Soc.* **2002**, *124*, 8186–8187.
- [46] C. E. Carraher, *J. Chem. Educ.* **1978**, *55*, 51–52.
- [47] C. E. French, S. Nicklin, N. C. Bruce, *J. Bacteriol.* **1996**, *178*, 6623–6627.
- [48] Bruker-AXS, *Proteum2*, Bruker AXS Inc., Madison, Wisconsin, USA, **2009**.
- [49] A. G. W. Leslie in *Joint CCP4 & ESRF-EACBM Newsletter on Protein Crystallography*, Vol. 26, Serc Laboratory, Daresbury, Warrington, **1992**.
- [50] Collaborative Computational Project Number 4, *Acta Crystallogr. Sect. D Biol. Crystallogr.* **1994**, *50*, 760–763.
- [51] A. Perrakis, R. Morris, V. S. Lamzin, *Nat. Struct. Biol.* **1999**, *6*, 458–463.
- [52] P. Emsley, K. Cowtan, *Acta Crystallogr. Sect. D Biol. Crystallogr.* **2004**, *60*, 2126–2132.

Received: November 2, 2010

Published online on March 4, 2011